

A Bayesian Meta-Analysis On Published Sample Mean and Variance

Pharmacokinetic Data

With Application To Drug-Drug Interaction Prediction

Menggang Yu¹, Seongho Kim¹, Zhiping Wang¹, Stephen Hall², and Lang Li^{1*}

¹Division of Biostatistics, Department of Medicine, School of Medicine, Indiana University, Indianapolis, IN, 46032;

²Division of Clinical Pharmacology, Department of Medicine, School of Medicine, Indiana University, Indianapolis, IN, 46032;

*Corresponding author email: lali@iupui.edu.

Summary: In drug-drug interaction (DDI) research, a two drug interaction is usually predicted by individual drug pharmacokinetics (PK). Although subject-specific drug concentration data from clinical PK studies on inhibitor/inducer or substrate's PK are not usually published, sample mean plasma drug concentrations and their standard deviations have been routinely reported. Hence there is a great need for meta-analysis and DDI prediction using such summarized PK data. In this paper, an innovative DDI prediction method based on a three-level hierarchical Bayesian meta-analysis model is developed for this purpose. Sample mean and variance are described by a level-one model; between-study variances are specified by a level-two model; and prior distributions are characterized by a level-three model. Through ketoconazole/midazolam example and simulations, we demonstrate that our meta-analysis model can not only estimate PK parameters, but also can recover their between-study/subject variances. Most importantly, the posterior distributions of PK parameters and their variance components allow us to predict DDI at both population-average and study-specific levels, so can we predict the DDI between-subject/study variance. These statistical predictions have never been investigated in a DDI research. Our simulation studies show that our meta-analysis approach has small bias in PK parameter estimates and DDI predictions. Sensitivity analysis was conducted to investigate the influences of PK parameters, such as an inhibition constant K_i , on the DDI prediction.

Keywords: area under the concentration curve ratio (*AUCR*), Bayesian hierarchical model, drug-drug interaction (DDI), meta-analysis, Monte Carlo Markov chain (MCMC), pharmacokinetics (PK), and prediction.

1. Introduction

Pharmacokinetic (PK) approaches designed to characterize drug to absorption, distribution and elimination are well established (Rowland and Tozer 1995) and robust statistical methodologies have been developed (Davidian and Giltinan 1995). Recently pharmacokinetic interactions among multiple drugs have received a great deal of attention because this phenomenon makes a significant contribution to adverse drug reaction profile of new drugs (Ito *et al.* 1998). The importance of drug-drug interactions (DDI) is exemplified by the interaction of ketoconazole and terfenadine, which caused potentially life-threatening ventricular arrhythmias (Monahan *et al.* 1990), and the interaction between sorivudine and fluorouracil which resulted in fatal toxicity (Watabe *et al.* 1996; Okuda *et al.* 1997).

In the DDI research, one of the central questions is whether two individual drugs' PK model and their *in-vitro* DDI parameters can predict their *in-vivo* DDI (Ito *et al.* 1998)? Since all the prior PK models and their parameters are summarized from multiple data sources (i.e. published PK studies in either literatures or public databases), and the data (i.e. drug concentrations) are usually published as sample mean profiles, together with standard deviations. This meta-analysis becomes particularly challenging, and there is a great need for such analysis based on summarized data.

Current statistical methods can neither fit PK models nor estimate PK parameters from sample mean data, nor evaluate the DDI prediction based on estimated PK models and parameters. Our pioneer work (Li *et al.* 2006) has developed a statistical model for DDI prediction based on sample mean data. Its focus was on estimating PK parameters. We have shown that it is feasible to draw inference for important PK parameters even with summarized data. This paper extends our previous work (Li *et al.* 2006) and aims at estimating both PK

parameters and variance components, and predicting the mean and variance of DDI, as the latter is more of an interest in a DDI PK study.

It is well known that the majority of DDIs depend on drug metabolizing enzymes and/or cell membrane drug transporters (www.Drug-Interactions.com). The single most important locus of DDIs is the cytochrome P450 (CYP) family of drug monooxygenases located in the gut-wall and liver (de Waziers *et al.* 1990). Among CYPs, CYP3A is the most abundant and accounts for approximately 30% and 90% of CYP protein the liver and intestine, respectively (Shimada *et al.* 1994). In addition, more than 60% of the drugs that are eliminated primarily by metabolism are metabolized by CYP3A. Ketoconazole (KETO) is a potent and extensively characterized CYP3A inhibitor, and midazolam (MDZ) is a highly selective CYP3A substrate *in vivo* that does not depend on membrane transporters for intracellular access (Tsunoda *et al.* 1999). Therefore, the KETO-MDZ pair is employed as an inhibitor-substrate example to illustrate our model based DDI prediction.

2 Specification of Models for Meta-analysis

2.1 PK Models

Table 1 and Figure 1 (a) summarize seven published KETO PK data sets that are used to establish the PK model of KETO. Some studies (Figure 1a) with longer blood sample collection times demonstrate biphasic decline in plasma concentrations consistent with a two compartment PK model (Gascoign *et al.* 1981; Huang *et al.* 1986; FDA 1999). Elimination of KETO occurs from the central compartment and systemic clearance is assumed to be equivalent to hepatic clearance. Table 1 and Figure 1 (b) summarize two published MDZ data sets. They are used to establish MDZ PK model and estimate its PK parameters. The MDZ PK is also assumed to

follow a two-compartment model with intravenous infusion. Specifically, we have the following differential equation based models

- PK model of KETO

$$\begin{aligned}\frac{dA_{1I}}{dt} &= F_I \times Dose \times ka_I \times e^{-ka_I t} - CL_I \times \frac{A_{1I}}{V1_I} + \left(-\frac{A_{1I}}{V1_I} + \frac{A_{2I}}{V2_I}\right) \times CL12_I, \\ \frac{dA_{2I}}{dt} &= \left(\frac{A_{1I}}{V1_I} - \frac{A_{2I}}{V2_I}\right) \times CL12_I, \quad (A_{1I}, A_{2I})|_{t=0} = (0,0).\end{aligned}\tag{1}$$

- PK model of MDZ

$$\begin{aligned}\frac{dA_{1S}}{dt} &= -CL_S \times \frac{A_{1S}}{V1_S} + \left(-\frac{A_{1S}}{V1_S} + \frac{A_{2S}}{V2_S}\right) \times CL12_S \\ \frac{dA_{2S}}{dt} &= \left(\frac{A_{1S}}{V1_S} - \frac{A_{2S}}{V2_S}\right) \times CL12_S, \quad (A_{1S}, A_{2S})|_{t=0} = (Dose,0).\end{aligned}\tag{2}$$

Here subscript *I* indicates the inhibitor, KETO, and subscript *S* represents substrate MDZ. F_I is the bioavailability which is assumed to be known, 0.7, (Cleary *et al.* 1992); ka_I is the absorption rate constant for KETO. There is no absorption rate constant and bioavailability parameters for MDZ as both MDZ PK studies followed the IV route. In both drug compounds, the volumes of distribution in systemic and peripheral compartments are ($V1, V2$) respectively and $CL12$ is the inter-compartment rate constant; CL is the hepatic (systemic) clearance, which is described by the well-stirred model $CL = Q_h \times CL_{int} / (Q_h + CL_{int})$, and hepatic blood-flow, $Q_h = 80$ l/h (Price *et al.* 2003) is known and the same for both KETO and MDZ. The intrinsic hepatic clearance is $CL_{int} = V \max / (Km + A1/V1)$. In particular, Km is assumed to be known for both KETO and MZD, i.e. $Km_I = 0.5$ and $Km_S = 2$.

2.2 Meta-analysis Models with Individual Level Data

Before describing various models, we use the following notations throughout our paper. The subscript i will be used for subject, j for time point, k for study and h for (dosing) phase. We assume that there are n_{kh} subjects in the dosing phase h of study k ; study k has H_k phases and there are total of K studies for a given drug. For ease of presentation, we assume all subjects within a dosing phase of a specific study are measured at the same time points to plasma concentration data, therefore we have T_{kh} time points in the dosing phase h of study k . A parameter without subscript will be a fixed effect parameter assumed invariant across studies while a parameter with subscript is a random effect parameter corresponding to the subscript. We also use bolded symbols for vectors and matrices. Hence for example, $\boldsymbol{\alpha}$ will be a vector of fixed effects whose values are invariant across different studies, $\boldsymbol{\beta}_{ik}$ is a vector of random subject specific parameter for subject i from study k .

When individual level data are available for each study, summarizing PK parameters from multiple sources by meta-analysis has been addressed by applying Bayesian methods to construct a drug PK model from several clinical study data sets. This model specification has been proposed in literature (Wakefield and Rahman 2000). In general, the following model is used

- subject-specific PK model:

$$p(y_{ijkh} | \boldsymbol{\alpha}, \boldsymbol{\beta}_{ik}, t_{jkh}) \sim N[f(\boldsymbol{\alpha}, \boldsymbol{\beta}_{ik}, t_{jkh}), \sigma_0^2], \quad (3)$$

- subject-specific PK parameter model:

$$p(\boldsymbol{\beta}_{ik} | \boldsymbol{\beta}_k, \boldsymbol{\Sigma}) \sim MVN(\boldsymbol{\beta}_k, \boldsymbol{\Sigma}), \quad (4)$$

- study-specific PK parameter model:

$$p(\boldsymbol{\beta}_k | \boldsymbol{\Omega}) \sim MVN(\boldsymbol{\beta}, \boldsymbol{\Omega}), \quad (5)$$

In this hierarchical model, $f(\boldsymbol{\alpha}, \boldsymbol{\beta}_{ik}, t_{jkh})$ denotes the predicted log-transformed drug concentration for subject i at j th time point from phase h of study k , while y_{ijkh} is the observed log-transformed drug concentration. Basically, f corresponds to (part of) a numerical solution at given time points from (1) and (2) given the fixed effect parameter $\boldsymbol{\alpha}$ and random effect $\boldsymbol{\beta}_{ik}$. So in the case that y_{ijkh} is the KETO concentration observed from the first compartment, then $f = \log(AI/VI)$ with AI solved from (1). The dimension of $\boldsymbol{\alpha}$ is p , of $\boldsymbol{\beta}_{ik}$, $\boldsymbol{\beta}_k$, and $\boldsymbol{\beta}$ is q . The measurement error variation, σ_0^2 , is assumed equal across studies. The variance components $\boldsymbol{\Sigma}$ and $\boldsymbol{\Omega}$ are for subject-specific and study-specific PK parameters.

However, published data are often available in the form of sample average plasma drug concentration. In other words, only $(\bar{y}_{\bullet jkh}, s_{jkh}^2)$, in stead of y_{ijkh} are published. The prescribed method needs y_{ijkh} , and they can not be directly implemented to perform meta-analysis in our case. Reconstructing a drug PK model from $(\bar{y}_{\bullet jkh}, s_{jkh}^2)$ needs a new meta-analysis formulation and different Bayesian sampling algorithm. In addition to estimation, our other major focus is to perform DDI prediction based on meta-analysis.

To this end, we develop in the following subsection an innovative hierarchical Bayesian meta-analysis model, and utilize a Monte Carlo Markov chain (MCMC) method for PK parameter estimation and DDI prediction.

2.3 Meta-analysis Models with Sample Mean and Standard Deviation Data

As individual data are not available, it is an unrealistic goal to estimate subject level PK parameters. The sample mean data $\bar{y}_{\bullet jkh}$ at most provide information about study specific PK parameters $\boldsymbol{\beta}_k$ and study to study variation parameters $\boldsymbol{\Omega}$. The sample variance data s_{jkh}^2 at most

provide information about between-subject heterogeneity parameter Σ . As a result, models based on (3) – (5) are only suitable when working on subject level data. When only sample mean and sample variance data are available, they need to be modified to make estimation feasible. In other words, the models should not involve β_{ik} . For this purpose, we adapt as follows.

By Taylor expansion at β_k , $f(\alpha, \beta_{ik}, t_{jkh})$ can be approximated as

$$f(\alpha, \beta_{ik}, t_{jkh}) \approx f(\alpha, \beta_k, t_{jkh}) + \frac{\partial f}{\partial \beta_k^T} (\beta_{ik} - \beta_k). \quad (6)$$

Instead of individual level PK model (3), we assume the following *approximate* model

$$p(y_{ijkh} | \alpha, \beta_{ik}, t_{ijkh}) \sim N \left(f(\alpha, \beta_k, t_{jkh}) + \frac{\partial f}{\partial \beta_k^T} (\beta_{ik} - \beta_k), \sigma_0^2 \right)$$

Now by conditioning on the trial level parameter vector β_k and other fixed effects, we have

$$p(\bar{y}_{\bullet jkh} | \alpha, \beta_k, \Sigma, \Omega, \sigma_0^2) \sim N \left(f(\alpha, \beta_k, t_{jkh}), \frac{\mathbf{F}_{jkh}^T \Sigma \mathbf{F}_{jkh} + \sigma_0^2}{n_{kh}} \right) \quad (7)$$

where $\mathbf{F}_{jkh} = \frac{\partial f}{\partial \beta_k^T}$.

To obtain the approximate distribution for sample variance,

$$s_{jkh}^2 = \sum_{i=1}^{n_{jkh}} (y_{ijkh} - \bar{y}_{\bullet jkh})^2 / (n_{jkh} - 1),$$

we use the known fact the normalized sample variance of m

i.i.d. normal variables has a chi-square distribution with degree of freedom $m-1$. Now by

conditioning (7) on the trial level parameter vector β_k and other fixed effects, we

$$\text{have } p(y_{ijkh} | \alpha, \beta_{ik}, \Sigma, \sigma_0^2, t_{ijkh}) \sim N \left(f(\alpha, \beta_k, t_{jkh}), \mathbf{F}_{jkh}^T \Sigma \mathbf{F}_{jkh} + \sigma_0^2 \right)$$

Hence $\frac{\sum_{i=1}^{n_{kh}} (y_{ijkh} - \bar{y}_{\cdot jkh})^2}{\mathbf{F}_{jkh}^T \boldsymbol{\Sigma} \mathbf{F}_{jkh} + \sigma_0^2} \sim \chi_{n_{kh}-1}^2$, or equivalently

$$\frac{(n_{kh} - 1)}{\mathbf{F}_{jkh}^T \boldsymbol{\Sigma} \mathbf{F}_{jkh} + \sigma_0^2} S_{jkh}^2 \sim \chi_{n_{kh}-1}^2 \quad (8)$$

Notice that (7) and (8) depend only on $\boldsymbol{\beta}_k$, $\boldsymbol{\Sigma}$, and σ_0^2 . Hence estimation of these parameters is feasible with mean and standard deviation data. Our estimation will be based on the following hierarchical models.

- sample mean PK model

$$p(\bar{y}_{\cdot jkh} | \boldsymbol{\alpha}, \boldsymbol{\beta}_k, \boldsymbol{\Sigma}, \sigma_0^2) \sim N\left(f(\boldsymbol{\alpha}, \boldsymbol{\beta}_k, t_{jkh}), \frac{\mathbf{F}_{jkh}^T \boldsymbol{\Sigma} \mathbf{F}_{jkh} + \sigma_0^2}{n_{kh}}\right) \quad (9)$$

- sample variance PK model

$$\frac{(n_{kh} - 1)}{\mathbf{F}_{jkh}^T \boldsymbol{\Sigma} \mathbf{F}_{jkh} + \sigma_0^2} S_{jkh}^2 \sim \chi_{n_{kh}-1}^2 \quad (10)$$

- study-specific PK parameter model:

$$p(\boldsymbol{\beta}_k | \boldsymbol{\Omega}) \sim MVN(\boldsymbol{\beta}, \boldsymbol{\Omega}), \quad (11)$$

2.4 Prior Specification and Posterior Distributions

Due to the nonlinear structure from PK models (1) - (2), no conjugate priors exists for all parameter except $\boldsymbol{\Omega}$. Vague prior are used for PK parameter population level fixed effects $\boldsymbol{\alpha}$, and subject level heterogeneity parameter, $(\boldsymbol{\Sigma}, \boldsymbol{\Omega}, \sigma_0^2)$, where $\boldsymbol{\Sigma} = \text{diag}\{\sigma_l^2\}$ and $\boldsymbol{\Omega} = \text{diag}\{\omega_l^2\}$.

$$p(\boldsymbol{\alpha}, \boldsymbol{\beta}) = U(0, 10^4); \quad p(\sigma_l^2) = U(a, b) \Leftrightarrow p(\sigma_l^{-2}) = \frac{(\sigma_l^{-2})^{-2}}{(b-a)}, l = 0, 1, \dots, q; \quad (12)$$

$$p(\omega_l^2) = U(a, b) \Leftrightarrow p(\omega_l^{-2}) = \frac{(\omega_l^{-2})^{-2}}{(b-a)}, l = 1, \dots, q.$$

Variance components all follow a uniform prior because practically it rarely exceeds the bound

$$(a, b) = (0.01^2, 2^2).$$

Let $\bar{\mathbf{Y}}_{\bullet} = \{\bar{y}_{\bullet jkh}; j = 1, \dots, J; k = 1, \dots, K; h = 1, \dots, H\}$ be the sample mean data and

$\mathbf{S} = \{s_{jkh}^2; j = 1, \dots, J; k = 1, \dots, K; h = 1, \dots, H\}$ be the sample variance data. Then, the posterior

probability distribution based on (9) - (12) is,

$$\begin{aligned} & p(\boldsymbol{\alpha}, \boldsymbol{\beta}_1, \dots, \boldsymbol{\beta}_K, \boldsymbol{\Sigma}, \boldsymbol{\Omega}, \sigma_0^2 \mid \bar{\mathbf{Y}}_{\bullet}, \mathbf{S}) \\ & \propto \left\{ \prod_{k=1}^K \prod_{h=1}^{h_k} \prod_{j=1}^{n_{kh}} N \left(\bar{y}_{\bullet jkh} \mid f(\boldsymbol{\alpha}, \boldsymbol{\beta}_k, t_{jkh}), \frac{\mathbf{F}_{jkh}^T \boldsymbol{\Sigma} \mathbf{F}_{jkh} + \sigma_0^2}{n_{kh}} \right) \right\} \\ & \times \left\{ \prod_{k=1}^K \prod_{h=1}^{h_k} \prod_{j=1}^{n_{kh}} \chi^2_{n_{kh}-1} \left(\frac{(n_{kh} - 1) s_{jkh}^2}{\mathbf{F}_{jkh}^T \boldsymbol{\Sigma} \mathbf{F}_{jkh} + \sigma_0^2} \right) \right\} \\ & \left\{ \prod_{k=1}^K p(\boldsymbol{\beta}_k \mid \boldsymbol{\beta}, \boldsymbol{\Omega}) \right\} \times p(\boldsymbol{\alpha}, \boldsymbol{\beta}) \times p(\boldsymbol{\Sigma}) \times p(\boldsymbol{\Omega}) \times p(\sigma_0^2) \end{aligned} \quad (13)$$

The estimation procedure is implemented with a Monte Carlo Markov chain process. The posterior probability functions, $p(\boldsymbol{\beta} \mid \bullet)$, $p(\boldsymbol{\alpha} \mid \bullet)$, $p(\boldsymbol{\beta}_k \mid \bullet)$, $p(\sigma_0^{-2} \mid \bullet)$, $p(\sigma_i^{-2} \mid \bullet)$, and $p(\omega_i^{-2} \mid \bullet)$ are derived in the Appendix. In particular, $p(\boldsymbol{\alpha} \mid \bullet)$, $p(\boldsymbol{\beta}_k \mid \bullet)$, $p(\sigma_0^{-2} \mid \bullet)$, and $p(\sigma_i^{-2} \mid \bullet)$ are drawn through the Metropolis Hasting (MH) algorithm (Hastings 1970), as their explicit distribution forms are difficult to draw directly. Specifically, a random walk chain is used and the random step is taken to mean normal with mean 0 and standard deviation of 10%. The mixing is well with such proposed density and the acceptance rate varies. For population parameter $\boldsymbol{\alpha}$, the acceptance rate is about 40% and for most of the study specific parameters $\boldsymbol{\beta}_k$, the acceptance rates are close to 25%. Five independent chains were run simultaneously to determine the convergence with dispersed starting values on population parameters. It needed less than 4000 iterations for the estimated potential scale reduction criterion of Gelman and Rubin (1992) to be

less than 1.2. By visual inspection of traceplots, almost all chains start to mix well after 500 iterations. The final results are based on a single chain of 50000 iterations after a burn-in of 10000. Every 10th iteration after burn-in was extracted for summarizing results. The numerical strategies for solutions of the differential equations and the derivatives of differential equations are discussed in our early work (Li *et al.* 2002; Li *et al.* 2004). Both MCMC algorithms and numerical solutions of differential equations are implemented in the statistical freeware R 2.0.1.

2.5 An Alternative Bayesian Hierarchical Model for the Sample Mean PK Profile

In our previous work (Li *et al.* 2006), a three level hierarchical model was proposed to recover PK parameters from published sample mean data.

$$p(y_{\bullet jkh} | s_{jkh}^2, t_{jk}, \boldsymbol{\alpha}, \boldsymbol{\beta}_k) \cong N[f(t_{jk}, \boldsymbol{\alpha}, \boldsymbol{\beta}_k), s_{jkh}^2/n_k]. \quad (14)$$

$$p(\boldsymbol{\beta}_k | \boldsymbol{\Omega}) \sim MVN(\boldsymbol{\beta}, \boldsymbol{\Omega}), \quad (15)$$

$$p(\boldsymbol{\alpha}, \boldsymbol{\beta}) = U(0, 10^4),$$

$$p(\omega_l^2) = U(a, b) \Leftrightarrow p(\omega_l^{-2}) = \frac{(\omega_l^{-2})^{-2}}{(b-a)}, l = 1, \dots, q. \quad (16)$$

There are two major differences between models (9)-(12) and (14)-(16). Firstly, model (14) uses sample variance s_{jkh}^2/n_k to represent the variance of $y_{\bullet jkh}$, while model (9) selects its theoretical approximation, $(\mathbf{F}_{jkh}^T \boldsymbol{\Sigma} \mathbf{F}_{jkh} + \sigma_0^2)/n_{kh}$. Secondly, models (14)-(16) were not designed to recover the between-subject variance $\boldsymbol{\Sigma}$, while model (10) can. The MCMC algorithm for models (14)-(16) is in the Appendix IV of our previous work (Li *et al.* 2006). In the following context, (9)-(12) are referred as the mean-variance model, and (14)-(16) are referred as the mean model.

3 DDI Prediction

3.1 DDI PK Model

When KETO and MDZ are administrated separately, PK models (1), and (2), describe the plasma concentration time course, respectively, and these differential equations can be independently solved. However, when they are administrated simultaneously, (i.e. PO for KETO and IV for MDZ), the KETO PK model (1) and MDZ PK model (2) are connected by

$$CL_{\text{int},S} = \frac{V \max_S}{Km_S \times \left(1 + \frac{fu_I \times A1_I}{MW_I \times K_i \times V1_I}\right) + \frac{A1_S}{V1_S}}, \quad (17)$$

and they need to be jointly solved. In equation (17), $fu_I=0.03$ (Martinez-Jorda *et al.* 1990) is the unbound fraction of KETO in plasma, K_i is the inhibition constant parameter estimated *in vitro* using human liver microsomes, and $MW_I=0.53$ is the molecular weight of the inhibitor. Note that, the inhibition model (17) depends on $1/K_i$. Model (17) reduces to

$CL_{\text{int},S} = V \max_S / (Km_S + A1_S / V1_S)$ when there is no inhibitor (or KETO). A common criterion to evaluate the extent of interaction is the *AUC* ratio (*AUCR*) of substrate after and before inhibitor administration.

$$AUCR = \frac{AUC_{S,W}}{AUC_{S,WO}} = \frac{\int_0^{\infty} A_S(\mathbf{\alpha}, \mathbf{\beta}, K_i, t) dt}{\int_0^{\infty} A_S(\mathbf{\alpha}, \mathbf{\beta}, t) dt}, \quad \text{and} \quad \tilde{AUCR}(\mathbf{\alpha}, \mathbf{\beta}, K_i) = \frac{\tilde{AUC}_{S,W}(\mathbf{\alpha}, \mathbf{\beta}, K_i)}{\tilde{AUC}_{S,WO}(\mathbf{\alpha}, \mathbf{\beta}, K_i)} \quad (18)$$

where, $AUC_{S,W}$ is the substrate *AUC* with inhibitor, $AUC_{S,WO}$ is its *AUC* without inhibitor,

$(\tilde{AUC}_{S,W}, \tilde{AUC}_{S,WO})$ are *AUC* estimates based on the trapezoid rule (Rowland and Tozer 1995),

and $(\mathbf{\alpha}, \mathbf{\beta})$ are combined MDZ and KETO PK parameter vectors. For the sake of simplicity,

denote $AUCR(\mathbf{\alpha}, \mathbf{\beta}, K_i) = \tilde{AUCR}(\mathbf{\alpha}, \mathbf{\beta}, K_i)$.

In the early drug development stage, a decision of continuing clinical trials for a candidate drug partially depends on its interaction with the other drugs (inducers or inhibitors). PK model based DDI prediction becomes critical, and precise prediction can guide drug development. Practically, inhibitor's PK model and its PK parameters are estimated from its PK studies, substrate's PK model and parameters are estimated from substrate's PK studies, and their interaction parameters in (17) are measured from *in-vitro* studies. Then, DDI are predicted by the joint model from (1), (2), and (17). Please note that, the interaction model (17) and its parameters are not estimated from PK studies.

This model based DDI prediction has been successfully implemented for simulating and predicting the effect of non-simultaneous drug and inhibitor administration (Yang *et al.* 2003), but every PK parameters were treated as known without uncertainty in their DDI prediction. From the statistical point of view, this approach is incomplete, because PK parameters of inhibitor and substrate estimated from published studies must have standard error, and these uncertainties need to be translated into their DDI prediction, which has not been done. On the other hand, some interaction parameters measured from *in vitro* studies, such as K_i , didn't have reported standard error. That doesn't mean that K_i was 100% accurately estimated, and their sensitivity to DDI prediction needs to be evaluated. As a matter of fact, K_i is recommended to be between 0.18 and 0.0037 (<http://www.fda.gov/cber/gdlms/interaction.pdf>). It is worthwhile to check how sensitive of our model prediction (note: it is an *in vivo* prediction) is due to K_i .

3.2 DDI Prediction Based on Sample Mean and Standard Deviation Data

Population Average DDI Prediction

Denote $AUCR(\boldsymbol{\alpha}, \boldsymbol{\beta}, K_i)$ as the population average DDI. Based on posterior distributions of PK parameters from the mean-variance model, we are able to obtain a predictive distribution of $AUCR$ at the population-average level.

$$p[AUCR(\boldsymbol{\alpha}, \boldsymbol{\beta}, K_i) | \bar{\mathbf{Y}}_., \mathbf{S}] = \int p[AUCR(\boldsymbol{\alpha}, \boldsymbol{\beta}, K_i) | \boldsymbol{\alpha}, \boldsymbol{\beta}] p(\boldsymbol{\alpha}, \boldsymbol{\beta} | \bar{\mathbf{Y}}_., \mathbf{S}) d\boldsymbol{\alpha} d\boldsymbol{\beta} \quad (19)$$

This distribution can be sampled by $\{AUCR^{(u)} = AUCR(\boldsymbol{\alpha}^{(u)}, \boldsymbol{\beta}^{(u)}, K_i)\}_{u=1, \dots, U}$,

where $\{\boldsymbol{\alpha}^{(u)}, \boldsymbol{\beta}^{(u)}\}_{u=1, \dots, U}$ are their posterior draws. A sample size of $U=1000$ is sufficiently large.

Subject-Specific DDI Prediction

The subject-specific DDI is defined as $AUCR(\boldsymbol{\alpha}, \boldsymbol{\beta}_{ik}, K_i)$. Please note that the subscript i of

$\boldsymbol{\beta}_{ik}$ represents subject i , while K_i is a conventional term for the inhibition constant, and its

subscript represents inhibition. Please forgive us for this confusion. $AUCR(\boldsymbol{\alpha}, \boldsymbol{\beta}_{ik}, K_i)$'s posterior distribution is

$$\begin{aligned} & p[AUCR(\boldsymbol{\alpha}, \boldsymbol{\beta}_{ik}, K_i) | \bar{\mathbf{Y}}_., \mathbf{S}] \\ &= \int p[AUCR(\boldsymbol{\alpha}, \boldsymbol{\beta}_{ik}, K_i) | \boldsymbol{\alpha}, \boldsymbol{\beta}_{ik}] p(\boldsymbol{\beta}_{ik} | \boldsymbol{\beta}_k, \boldsymbol{\Sigma}) p(\boldsymbol{\beta}_k | \boldsymbol{\beta}, \boldsymbol{\Omega}) p(\boldsymbol{\alpha}, \boldsymbol{\beta} | \bar{\mathbf{Y}}_., \mathbf{S}) \\ & \times p(\boldsymbol{\Omega} | \bar{\mathbf{Y}}_., \mathbf{S}) p(\boldsymbol{\Sigma} | \bar{\mathbf{Y}}_., \mathbf{S}) d\boldsymbol{\alpha} d\boldsymbol{\beta} d\boldsymbol{\beta}_k d\boldsymbol{\Omega} d\boldsymbol{\Sigma}, \end{aligned} \quad (20)$$

and this distribution can be sampled by

$$\{AUCR^{(u)} \sim AUCR(\boldsymbol{\alpha}^{(u)}, \boldsymbol{\beta}^{(u)}, \boldsymbol{\beta}_k^{(u)}, \boldsymbol{\beta}_{ik}^{(u)}, \boldsymbol{\Omega}^{(u)}, \boldsymbol{\Sigma}^{(u)}, K_i)\}_{u=1, \dots, U}, \quad (21)$$

where $\{\boldsymbol{\alpha}^{(u)}, \boldsymbol{\beta}^{(u)}, \boldsymbol{\beta}_k^{(u)}, \boldsymbol{\beta}_{ik}^{(u)}, \boldsymbol{\Omega}^{(u)}, \boldsymbol{\Sigma}^{(u)}\}_{u=1, \dots, U}$ are their posterior draws. A sample size of $U = 1000$

is sufficiently large. Both population-average and subject-specific DDI predictions are

improvements over the deterministic approach (Yang *et al.* 2003), in which $(\boldsymbol{\alpha}, \boldsymbol{\beta})$ were chosen as

a set of fixed numbers (i.e. their estimates), and their estimation error and between-study/subject variation information were totally ignored.

DDI Variation Prediction

The other interesting statistic is the between-subject/study variance of DDI, which reflects the heterogeneity of DDI within the population. In the distribution of subject-specific DDI, $p[AUCR(\boldsymbol{\alpha}, \boldsymbol{\beta}_{ik}, K_i) | \bar{\mathbf{Y}}_i, \mathbf{S}]$, its posterior variance contains not only between-subject/study variances, but also uncertainty of PK parameters and their variance components estimates. Hence the variance of subject-specific $AUCR$'s prediction is higher than the between-subject/study variance of DDI, and it doesn't give us its distribution. Based on this consideration, a standard deviation statistic (23) is constructed from the following distribution (22),

$$\begin{aligned} & p[AUCR(\boldsymbol{\alpha}, \boldsymbol{\beta}_{ik}, K_i) | \boldsymbol{\Omega}, \boldsymbol{\Sigma}] \\ &= \int p[AUCR(\boldsymbol{\alpha}, \boldsymbol{\beta}_{ik}, K_i) | \boldsymbol{\beta}_i, \boldsymbol{\beta}_{ik}] p(\boldsymbol{\beta}_{ik} | \boldsymbol{\beta}_k, \boldsymbol{\Sigma}) p(\boldsymbol{\beta}_k | \boldsymbol{\beta}, \boldsymbol{\Omega}) d\boldsymbol{\beta}_k d\boldsymbol{\beta}_{ik}, \end{aligned} \quad (22)$$

$$\begin{aligned} & \hat{SD}[AUCR(K_i, \boldsymbol{\alpha}, \boldsymbol{\beta}, \boldsymbol{\Sigma}, \boldsymbol{\Omega})] \\ &= \text{standard deviation of } \{AUCR(\boldsymbol{\alpha}, \boldsymbol{\beta}, \boldsymbol{\beta}_i^{(v)}, \boldsymbol{\beta}_{ik}^{(v)}, K_i | \boldsymbol{\Sigma}, \boldsymbol{\Omega})\}_{v=1, \dots, V}, \end{aligned} \quad (23)$$

where $(\boldsymbol{\beta}_k^{(v)}, \boldsymbol{\beta}_{ik}^{(v)})$ are draws from $p(\boldsymbol{\beta}_{ik} | \boldsymbol{\beta}_k, \boldsymbol{\Sigma})$ and $p(\boldsymbol{\beta}_k | \boldsymbol{\beta}, \boldsymbol{\Omega})$ respectively. Consequently the distribution of $\hat{SD}[AUCR(K_i, \boldsymbol{\alpha}, \boldsymbol{\beta}, \boldsymbol{\Sigma}, \boldsymbol{\Omega}) | \bar{\mathbf{Y}}_i, \mathbf{S}]$ becomes

$$\begin{aligned} & p\{\hat{SD}[AUCR(K_i, \boldsymbol{\alpha}, \boldsymbol{\beta}, \boldsymbol{\Sigma}, \boldsymbol{\Omega}) | \bar{\mathbf{Y}}_i, \mathbf{S}]\} \\ &= \int \hat{SD}[AUCR(K_i, \boldsymbol{\alpha}, \boldsymbol{\beta}, \boldsymbol{\Sigma}, \boldsymbol{\Omega})] p(\boldsymbol{\alpha}, \boldsymbol{\beta} | \bar{\mathbf{Y}}_i, \mathbf{S}) p(\boldsymbol{\Sigma} | \bar{\mathbf{Y}}_i, \mathbf{S}) p(\boldsymbol{\Omega} | \bar{\mathbf{Y}}_i, \mathbf{S}) d\boldsymbol{\alpha} d\boldsymbol{\beta} d\boldsymbol{\Sigma} d\boldsymbol{\Omega}, \end{aligned} \quad (24)$$

and this distribution can be sampled from

$$\{\hat{SD}^{(u)} = \hat{SD}[AUCR(K_i, \boldsymbol{\alpha}^{(u)}, \boldsymbol{\beta}^{(u)}, \boldsymbol{\Sigma}^{(u)}, \boldsymbol{\Omega}^{(u)})]\}_{u=1, \dots, U}, \quad (25)$$

where $\{\boldsymbol{\alpha}^{(u)}, \boldsymbol{\beta}^{(u)}, \boldsymbol{\Sigma}^{(u)}, \boldsymbol{\Omega}^{(u)}\}_{u=1, \dots, U}$ are their posterior draws. A sample size of $U=V=1000$ is sufficiently large for us to obtain a posterior distribution of $\hat{SD}[AUCR(K_i)]$.

4. KETO/MDZ Example

The PK parameters of both KETO and MDZ are estimated from published studies using the proposed mean-variance model, as well as mean-model. The predicted log-transformed drug concentrations for KETO are calculated from the differential equation model (1) and the predicted log-transformed drug concentrations for MDZ are calculated from the differential equation model (2). Then, assuming known DDI parameters, $(K_{m_I}, K_{m_S}, f_{I_j}, K_i, MW_I)$, and the posterior distributions of the PK parameters of the two drugs, and the DDI outcome, $AUCR$, is predicted by model (1) and (2) linked by (17).

4.1 KETO Data Analysis

Table 1 and Figure 1 (a) summarize seven published KETO PK data sets that were used to establish the PK model of KETO. All studies employed oral (PO) dosing of the Nizoral (Janssen Pharmaceuticals) formulation of KETO was used in all seven studies. The participants in these seven studies were young and healthy. The KETO's mean-variance model is reformulated in order to facilitate our analysis illustration. Denoting subscript I as inhibitor KETO, the model is defined as following:

$$\begin{aligned}
 p(\bar{y}_{.jkh} | \boldsymbol{\alpha}, \boldsymbol{\beta}_k, \boldsymbol{\Sigma}, \boldsymbol{\Omega}, \sigma_0^2) &\sim N\left(f(\boldsymbol{\alpha}, \boldsymbol{\beta}_k, t_{jkh}), \frac{\mathbf{F}_{jkh}^T \boldsymbol{\Sigma} \mathbf{F}_{jkh} + \sigma_0^2}{n_{kh}}\right), \\
 \frac{(n_{kh} - 1)}{\mathbf{F}_{jkh}^T \boldsymbol{\Sigma} \mathbf{F}_{jkh} + \sigma_0^2} S_{jkh}^2 &\sim \chi_{n_{kh}-1}^2, \quad \boldsymbol{\Sigma} = \text{diag}(\sigma_1^2), \\
 \boldsymbol{\beta}_k &= (V1_{I,k}, V2_{I,k}, CL12_{I,k}, V \max_{I,k}, ka_{I,TM,k})^T, \\
 \boldsymbol{\alpha} &= (\Delta ka_{I,TF}, \Delta ka_{I,SLM}, \Delta ka_{I,SPF}, \Delta ka_{I,SLF})^T, \\
 V1_{I,k} &\sim N(V1_I, \omega_{I,1}^2), \quad V2_{I,k} \sim N(V2_I, \omega_{I,2}^2), \\
 CL12_{I,k} &\sim N(CL12_I, \omega_{I,3}^2), \quad V \max_{I,k} \sim N(V1_I, \omega_{I,4}^2), \\
 ka_{I,TM,k} &\sim N(ka_{I,TM}, \omega_{I,5}^2), \quad ka_{I,route} \sim ka_{I,TM} + 1_{route} \times \Delta ka_{I,route},
 \end{aligned} \tag{26}$$

where mean function $f(.) = AI_I/VI_I$ is solved from its PK model (1); Oral formulations included tablet, suspension and solution under fasting or meal conditions, hence the subscript of ka_I , route = (TM, TF, SPF, SLM, SLF). Model (26) assumes that the $ka_{I, TM}$'s relative differences to the other rates, $(\Delta ka_{I, TF}, \Delta ka_{I, SLM}, \Delta ka_{I, SPF}, \Delta ka_{I, SLF})$, are fixed. In addition, all the random effects in model (26) are independent. The PK parameters are log-transformed, hence the interpretation of all the variance components is coefficient of variance (CV). The prior distributions follow the same formulations as those in (12). On the other hand, the mean-model of KETO is almost the same as (26), and the only difference is that it has a sample mean model (14).

In our MCMC algorithm, a total of 50000 iterations were run and 10000 were used as burn-in. To avoid autocorrelations among these draws, we picked every 10th sample for summarizing results. They are reported in Table 2 and Figure 2. The 90% credit intervals of PK parameters are presented at their relative scales to their means. Here are some highlights.

- Among the KETO PK parameter estimates, $V2_I$ and $CL12_I$ have wider 90% CI than the others. This is because only three studies (Gascoigne *et al.* 1981; Huang *et al.* 1986; and FDA 1999) had sampling time points late enough to detect the terminal phase of KETO elimination from plasma, while the other studies did not.
- $V2_I$ and $CL12_I$'s between-study CV estimates, 0.64 and 0.72 respectively, are larger than the other between-study CV estimates.
- The between-subject CV is estimated to be the same among all PK parameters in model (26). Its example fitting to sample variances is illustrated by Figure 2(a) for a KETO study (Gascoigne *et al.* 1981). The between-subject CV is estimated 0.49, and the within subject CV is estimated as 0.10.

- Both mean-variance model (model 2 in table 2) and mean-model (model 1) have comparable performance in estimating PK parameters and their between-study CVs.

4.2 MDZ Data Analysis

Table 1 and Figure 1 (b) summarize two published MDZ data sets. They were used to establish MDZ's PK model and estimate its PK parameters. Midazolam (administered as Versed®, Roche Pharmaceuticals) was administered in the fasting state in all studies. The participants in these two studies were young and healthy. Denoting subscript S as substrate MDZ, its mean-variance model is as following:

$$\begin{aligned}
 p(\bar{y}_{\cdot jkh} | \boldsymbol{\beta}_k, \boldsymbol{\Sigma}, \boldsymbol{\Omega}, \sigma_0^2) &\sim N\left(f(\boldsymbol{\beta}_k, t_{jkh}), \frac{\mathbf{F}_{jkh}^T \boldsymbol{\Sigma} \mathbf{F}_{jkh} + \sigma_0^2}{n_{kh}}\right), \\
 \frac{(n_{kh} - 1)}{\mathbf{F}_{jkh}^T \boldsymbol{\Sigma} \mathbf{F}_{jkh} + \sigma_0^2} s_{jkh}^2 &\sim \chi_{n_{kh} - 1}^2, \quad \boldsymbol{\Sigma} = \text{diag}(\sigma_1^2), \\
 \boldsymbol{\beta}_k &= (V1_{S,k}, V2_{S,k}, CL12_{S,k}, V \max_{S,k})^T, \\
 V1_{S,k} &\sim N(V1_S, \omega_S^2), \quad V2_{S,k} \sim N(V2_S, \omega_S^2), \\
 CL12_{S,k} &\sim N(CL12_S, \omega_S^2), \quad V \max_{S,k} \sim N(V1_S, \omega_S^2).
 \end{aligned} \tag{27}$$

where mean function $f(\cdot) = A1_S / V1_S$ is solved from its PK model (2). The prior distributions follow the same formulations as those in (12). Model (27) assumes the same between-study CV for all PK parameters, because only two studies are available. The mean-model of MDZ is almost the same as (27), and the only difference is that it has a sample mean model (14). In our MCMC algorithm, a total of 50000 iterations were run and 10000 were used as burn-in. To avoid autocorrelations among these draws, we pick every 10th sample for summarizing results. They are reported in Table 2. Here are some highlights.

- All of MDZ PK parameter estimates have comparable 90% CIs.

- The between-study CV is estimated as 0.32, between-subject CV is estimated as 0.14, and the within subject CV is estimated as 0.10. The fitting of sample variance is displayed by an MDZ example (Lee *et al.* 2002) in Figure 2(b).
- Both mean-variance model (model 2 in table 2) and mean-model (model 1) have comparable performance in estimating PK parameters and their between-study CVs.

4.3 KETO/MDZ Interaction Prediction

Assuming a simultaneous oral dose KETO and an IV dose for MDZ, the interaction PK models follow equations (1) and (2) connected by (17), in which K_i is assumed to take value of (0.0037, 0.01, 0.18) μM to assess its sensitivity in DDI prediction. In the simulation, the blood sampling time points are (0.25, 0.5, 1, 1.5, 2, 3, 4, 6, 12) hours after dose. MDZ is dosed at (2, 5, 10) mg levels, and KETO/MDZ is dosed at three combinations: 200/2mg, 400/5mg, 800/10mg. The predicted MDZ plasma concentrations are simulated both with and without KETO, and at three different K_i values. AUC and $AUCR$ are calculated with the trapezoid rule (Rowland and Tozer 1995). Following our proposed DDI prediction procedures in section 3.2, population-average DDI, subject-specific DDI, and between-subject/study variance of DDI are predicted and displayed in Table 3. Here are some highlights.

- The smaller the K_i , the larger the predicted $AUCR$. The larger the dose combination, the larger the predicted $AUCR$. These results fit well to previous simulation studies (Yang *et al.* 2003).
- The smaller the K_i , the smaller between-subject/study CV. The larger the dose combination, the larger the CVs of population-average and subject-specific $AUCR$ s.

- Subject-specific *AUCR* and population-average *AUCR* have very comparable mean estimate, but subject-specific *AUCR* has much higher CVs, which is due to the additional between-subject/study variations.
- The predicted mean between-subject/study CV is smaller than the CV of the subject-specific *AUCR*, because it doesn't contain the variability due to the uncertainties of PK parameter estimates.

5. Simulation Studies for PK Parameter Estimation and DDI Prediction

Based on our proposed hierarchical Bayesian model, sample mean drug concentration data and their sample variances were fitted to estimate PK parameters and variance components for KETO and MDZ. It is not clear whether the estimates are biased, and consequently whether the predicted *AUCR* and its variance are biased? To answer these questions, statistical simulations were conducted. In short, separate KETO and MDZ PK trials were simulated at different doses. Subject-specific level drug concentrations were obtained and the sample means and standard deviations were summarized. Then PK models were fitted to the sample mean and standard deviation data to estimate KETO and MDZ's PK parameters and variance components' posterior distributions.

In each simulation data set, eight studies for both KETO and MDZ were generated. Each study had 3 tablet dose levels with meals. There were 24 subjects for each study. Individual data were simulated first and then summarized as mean and standard deviation data for analysis. The blood sampling time points were (0.25, 0.5, 1, 1.5, 2, 3, 4, 6, 12, 24, 36) hours after dose for KETO and (0.25, 0.5, 1, 1.5, 2, 3, 4, 6, 12) for MDZ. KETO was dosed at (200, 400, 800) mg levels, MDZ was dosed at (2, 5, 10) mg levels.

Specifically, in each KETO dose, its subject specific plasma concentrations were simulated with a two-compartment model (1) and statistical model (26). The population PK parameters are $\boldsymbol{\beta} = \log(V1_I, V2_I, CL12_I, V \max_I, ka_{I, TM})$. We utilized the similar PK parameters from prescribed data analysis as their true values (Table 2). The between subject variance matrix is taken as $\sigma_1^2 I_{5 \times 5}$ with σ_1^2 set to be 0.20^2 . Study to study variance matrix is taken as $\omega_1^2 I_{5 \times 5}$ with ω_1^2 set to be 0.30^2 . The measurement error variance σ_0^2 is set as 0.10^2 .

Similar to the KETO dose, a MDZ dose was simulated with a two compartmental PK model (2) and statistical model (27). The PK parameters are $\boldsymbol{\beta} = \log(V1_S, V2_S, V \max_S, CL12_S)$, and the true PK parameters are listed in Table 3 and are chosen to be close to their estimates in the prescribed MDZ data analysis. The between subject variance matrix is taken as $\sigma_1^2 I_{4 \times 4}$ with σ_1^2 set to be 0.20^2 . Study to study variance matrix is taken as $\omega_1^2 I_{4 \times 4}$ with ω_1^2 set to be 0.30^2 . The measurement error variance σ_0^2 is set as 0.10^2 . Totally, 100 simulated data sets were generated for both KETO and MDZ under each dose.

To fit the PK model in each simulation data set, an M-H algorithm was implemented as in the data example. To save computation time, initial values for PK parameters and variance components were chosen as their true values plus random noise with a coefficient of variation of approximately 10%. This can certainly increase the convergence rate of the algorithm, yet has minimum impact for the convergence itself. Total of 3000 iterations with 1000 burn-in were run to obtain PK parameter posterior distributions after the MCMC reached convergence. One in every five samples was picked to avoid autocorrelations. Both mean-variance model and mean-model were fitted to simulated data sets. Table 4 summarizes the PK parameters and variance components estimation biases for both approaches. Figure 3 summarizes the simulation results

for *AUCR* prediction; and Figure 4 summarizes the *AUCR*'s variation prediction. Here are the highlights.

- In Table 4, except that *CL12*'s relative bias is around 7.5%, all the other PK parameters have relative bias less than 5%. *CL12* and *V2*'s estimates have larger bias than the other PK parameters. It is true in both mean-variance model and mean-model.
- In Table 4, both the between-subject and between-study variances are estimated with less than 5% relative bias.
- In Figure 3, both subject-specific and population-average *AUCR* predictions have bias less than 5%. Their 90% CI coverage probabilities are close to their nominal levels.
- In Figure 4, *AUCR*'s between-subject/study variation predictions have bias less than 5%, and their 90% CI coverage probabilities are close to their nominal levels.

6. Conclusions

In this paper, we propose a DDI prediction method based on an innovative three level hierarchical Bayesian model to reconstruct a drug's PK model from multiple published PK studies. This approach can not only estimate PK parameters, but also can recover their between-study/subject variations. Most importantly, the posterior distributions of PK parameters and their variance components allow us to predict DDI at both population-average and study-specific levels, so can we predict the DDI between-subject/study variance. These statistical predictions have never been investigated in a DDI research. Our simulation studies show that our meta-analysis approach has small bias in PK parameter estimates and DDI prediction, when using the published sample mean and variance data.

Both data analysis and simulation studies demonstrate that mean-variance model proposed in this paper and our previous work (Li *et al.* 2006), mean-model, have very comparable performances in PK parameter estimations. In our previous work (Li *et al.* 2006), it was shown that our prior distribution selection, model (12), was not sensitive to PK parameter estimation. In addition, a two-order Taylor expansion approximate in (9) did not reduce the bias much (Li *et al.* 2006). This is consistent with that of the marginal quasi-likelihood (MQL) approach in generalized linear mixed model (Molenberghs and Verbeke, 2005, Chapter 14, page 270-273). Other approximation method, such as penalized quasi-likelihood approach (PQL) was reported to have better performance (Breslow and Clayton 1993; Wolfinger 1993), which is a first order Taylor expansion around subject-specific parameters. However, as the subject-specific level PK parameter information is not available in the sample mean data, PQL approach is not applicable in our meta-analysis.

Our proposed approach has a great potential as a regular statistical tool in DDI research, since the summarized PK data from published resources are usually much more readily available than the subject-level raw data. The Bayesian model provides a flexible framework to integrate prior knowledge into the estimation and prediction procedures.

References

- Breslow, N. E., and Clayton, D. G. (1993). Approximate inference in generalized linear mixed models. *Journal of American Statistical Association* 88: 9-25.
- Cleary, J. D., Taylor, J. W., and Chapman, S. W. (1992). Itraconazole in antifungal therapy. *Ann Pharmacother* 26(4): 502-9.
- Daneshmend, T. K., Warnock, D. W., Ene, M. D., Johnson, E. M., Parker, G., Richardson, M. D., and Roberts, C. J. (1983). Multiple dose pharmacokinetics of ketoconazole and their effects on antipyrine kinetics in man. *J Antimicrob Chemother* 12(2): 185-8.
- Daneshmend, T. K., Warnock, D. W., Ene, M. D., Johnson, E. M., Potten, M. R., Richardson, M. D., and Williamson, P. J. (1984). Influence of food on the pharmacokinetics of ketoconazole. *Antimicrob Agents Chemother* 25(1): 1-3.
- Daneshmend, T. K., Warnock, D. W., Turner, A., and Roberts, C. J. (1981). Pharmacokinetics of ketoconazole in normal subjects. *Journal of Antimicrobial Chemotherapy* 8(299-304).
- Davidian, M., and Giltinan, D. M. (1995). *Nonlinear models for repeated measurement data*. New York, Chapman and Hall.
- de Waziers, I., Cugnenc, P. H., Yang, C. S., Leroux, J. P., and Beaune, P. H. (1990). Cytochrome P 450 isoenzymes, epoxide hydrolase and glutathione transferases in rat and human hepatic and extrahepatic tissues. *J Pharmacol Exp Ther* 253(1): 387-94.
- FDA. (1999). Bioequivalence Reviews. from http://www.fda.gov/cder/foi/anda/99/74-971_Ketoconazole.htm.
- Gascoigne E. W., Michaels M., Meuldermans W., and Heykants J. (1981). The kinetics of ketoconazole in animals and man. *Clinical Research Reviews* 1(3): 177-187.
- Gascoigne, E. W., Barton, G. J., Michaels, M., Meuldermans, W., and Heykants, J. (1981). The kinetics of ketoconazole in animals and man. *Clinical Research Reviews* 1(3): 177-187.
- Gelman, A., and Rubin, D. B. (1992). Inference From Iterative Simulation Using Multiple Sequences. *Statistical Science* 7: 457-472.
- Hastings, W. K. (1970). Monte Carlo Sampling Methods Using Markov Chains and Their Applications. *Biometrika* 57: 97-109.
- Huang, Y. C., Colaizzi, J. L., Bierman, R. H., Woestenborghs, R., and Heykants, J. (1986). Pharmacokinetics and dose proportionality of ketoconazole in normal volunteers. *Antimicrob Agents Chemother* 30(2): 206-10.
- Ito, K., Iwatsubo, T., Kanamitsu, S., Ueda, K., Suzuki, H., and Sugiyama, Y. (1998). Prediction of pharmacokinetic alterations caused by drug-drug interactions: metabolic interaction in the liver. *Pharmacol Rev* 50(3): 387-412.
- Lee, J. I., Chaves-Gnecco, D., Amico, J. A., Kroboth, P. D., Wilson, J. W., and Frye, R. F. (2002). Application of semisimultaneous midazolam administration for hepatic and intestinal cytochrome P450 3A phenotyping. *Clin Pharmacol Ther* 72(6): 718-28.
- Li, L., Brown, M. B., Lee, K. H., and Gupta, S. (2002). Estimation and inference for a spline-enhanced population pharmacokinetic model. *Biometrics* 58(3): 601-11.
- Li, L., Lin, X., Brown, M., Gupta, S., and Lee, K.H. (2004). A population pharmacokinetic model with time-dependent covariates measured with errors. *Biometrics* 60: 451-460.
- Li, L., Yu, M., Chin, R., Lucksiri, A., Flockhart, D., and Hall, S. (2006). Drug-Drug Interaction Prediction: A Bayesian Meta-Analysis Approach. *Statistics in Medicine* (accepted).

- Martinez-Jorda, R., Rodriguez-Sasianin, J. M., and Calvo, R. (1990). Serum Binding of Ketoconazole in Health and Disease. *International Journal fo Clinical Pharmacology Research* 5: 271-276.
- Molenberghs, G., and Verbeke, G. (2005). *Models for discrete Longintudinal data*.
- Monahan, B. P., Ferguson, C. L., Killeavy, E. S., Lloyd, B. K., Troy, J., and Cantilena, L. R. Jr. (1990). Torsades de pointes occurring in association with terfenadine use. *JAMA* 264(21): 2788-90.
- Okuda, H., Nishiyama, T., Ogura, K., Nagayama, S., Ikeda, K., Yamaguchi, S., Nakamura, Y., Kawaguchi, Y., and Watabe, T. (1997). Lethal drug interactions of sorivudine, a new antiviral drug, with oral 5-fluorouracil prodrugs. *Drug Metab Dispos* 25(5): 270-3.
- Price, P. S., Conolly, R. B., Chaisson, C. F., Gross, E. A., Young, J. S., Mathis, E. T., and Tedder, D. R. (2003). Modeling interindividual variation in physiological factors used in PBPK models of humans. *Crit Rev Toxicol* 33(5): 469-503.
- Rowland, M., and Tozer, T. N. (1995). *Clinical Pharmacokinetics Concept and Applications*. London, Lippincott Williams & Wilkins.
- Shimada, T., Yamazaki, H., Mimura, M., Inui, Y., and Guengerich, F. P. (1994). Interindividual variations in human liver cytochrome P-450 enzymes involved in the oxidation of drugs, carcinogens and toxic chemicals: studies with liver microsomes of 30 Japanese and 30 Caucasians. *J Pharmacol Exp Ther* 270(1): 414-23.
- Tsunoda, S. M., Velez, R. L., von Moltke, L. L., and Greenblatt, D. J. (1999). Differentiation of intestinal and hepatic cytochrome P450 3A activity with use of midazolam as an in vivo probe: effect of ketoconazole. *Clin Pharmacol Ther* 66(5): 461-71.
- Wakefield, J. C., and Rahman, N. (2000). The combination of population pharmacokinetic studies. *Biometrics* 56(1): 263-70.
- Watabe, T. (1996). Strategic proposals for predicting drug-drug interactions during new drug development: based on sixteen deaths caused by interactions of the new antiviral sorivudine with 5-fluorouracil prodrugs. *J Toxicol Sci* 21(5): 299-300.
- Wolfinger, R., and O'Connell, M (1993). Generalized linear mixed models: a pseudo-likelihood approach. *Journal of statistical Computation and Simulation*. 48: 233-243.
- Yang, J., Kjellsson, M., Rostami-Hodjegan, A., and Tucker, G. T. (2003). The effects of dose staggering on metabolic drug-drug interactions. *Eur J Pharm Sci* 20(2): 223-32.

Acknowledgement

Drs. Lang Li, Menggang Yu, and Stephen Hall's researches are supported by NIH grants, R01 GM74217 (LL), R01 GM67308 (SH), FD-T-001756(SH).

Appendix Posterior Distributions

The following functions are conditional distributions to draw PK parameters and their variance components parameters in our three level hierarchical Bayesian model proposed in section 3.

Data analysis proposed in section 4 also utilized the following distributions.

Population PK parameters $(\boldsymbol{\alpha}, \boldsymbol{\beta}=(\beta_1, \dots, \beta_q)^T)$ and study level PK parameters β_k :

$$p(\boldsymbol{\alpha} | \bullet) \propto \left\{ \prod_{h=1}^{H_k} \prod_{j=1}^{n_{kh}} N \left(f(\boldsymbol{\alpha}, \boldsymbol{\beta}_k, t_{jkh}), \frac{\mathbf{F}_{jkh}^T \boldsymbol{\Sigma} \mathbf{F}_{jkh} + \sigma_0^2}{n_{kh}} \right) \right\} \quad (\text{A1})$$

$$p(\boldsymbol{\beta}_k | \bullet) \propto \left\{ \prod_{h=1}^{H_k} \prod_{j=1}^{n_{kh}} N \left(f(\boldsymbol{\alpha}, \boldsymbol{\beta}_k, t_{jkh}), \frac{\mathbf{F}_{jkh}^T \boldsymbol{\Sigma} \mathbf{F}_{jkh} + \sigma_{0k}^2}{n_k} \right) \right\} \times \left\{ \prod_{k=1}^K p(\boldsymbol{\beta}_k | \boldsymbol{\beta}, \boldsymbol{\Omega}) \right\} \quad (\text{A2})$$

$$p(\beta_l | \bullet) \propto N \left(\left\{ \frac{1}{\tau_l^2} + \frac{K}{\omega_l^2} \right\}^{-1} \left\{ \frac{1}{\tau_l^2} \mu_l + \frac{K}{\omega_l^2} \bar{\beta}_{\cdot l} \right\}, \left\{ \frac{1}{\tau_l^2} + \frac{K}{\omega_l^2} \right\}^{-1} \right)$$

$$\text{for } l=1, \dots, q; \text{ where } \bar{\beta}_{\cdot l} = \sum_{k=1}^K \beta_{kl} \quad (\text{A3})$$

Variance components:

$$\text{Pr}(\omega_l^2 | \bullet) \sim \text{Inv - Gamma} \left[\left(\frac{K}{2} - 1 \right), \left(\frac{\sum_{k=1}^K (\beta_{kl} - \beta_l)^2}{2} \right) \right] \times 1_{\omega_l^2} (0.01^2, 2^2) \quad (\text{A4})$$

where $1_{\omega_l^2} (0.01^2, 2^2)$ equals 1 when ω_l^2 is inside $(0.01^2, 2^2)$ and 0 otherwise.

$$p(\sigma_l^2 | \bullet) \propto \prod_{k=1}^K \prod_{h=1}^{H_k} \prod_{j=1}^{n_{kh}} (\mathbf{F}_{jkh}^T \boldsymbol{\Sigma} \mathbf{F}_{jkh} + \sigma_0^2)^{-\frac{n_{kh}+1}{2}} \times \exp \left\{ - \frac{n_{kh} \{ \bar{y}_{\cdot jkh} - f(\boldsymbol{\alpha}, \boldsymbol{\beta}_k, t_{jkh}) \}^2 + \sum_{i=1}^{n_{kh}} (y_{ijkh} - \bar{y}_{\cdot jkh})^2}{2(\mathbf{F}_{jkh}^T \boldsymbol{\Sigma} \mathbf{F}_{jkh} + \sigma_0^2)} \right\} \times 1_{\sigma_l^2} (0.01^2, 2^2) \quad (\text{A5})$$

$$\begin{aligned}
& p(\sigma_0^2 | \bullet) \\
& \propto \prod_{k=1}^K \prod_{h=1}^{H_k} \prod_{j=1}^{n_{kh}} (\mathbf{F}_{jkh}^T \mathbf{F}_{jkh} \sigma_1^2 + \sigma_0^2)^{-\frac{n_{kh}+1}{2}} \\
& \times \exp \left\{ -\frac{n_{kh} \left\{ \bar{y}_{\bullet jkh} - f(\mathbf{a}, \mathbf{b}_k, t_{jkh}) \right\}^2 + \sum_{i=1}^{n_{kh}} (y_{ijkh} - \bar{y}_{\bullet jkh})^2}{2(\mathbf{F}_{jkh}^T \mathbf{F}_{jkh} \sigma_1^2 + \sigma_0^2)} \right\} \times 1_{\sigma_0^2}(0.01^2, 2^2)
\end{aligned} \tag{A6}$$

Here $1_{\sigma_1^2}(0.01^2, 2^2)$ and $1_{\sigma_0^2}(0.01^2, 2^2)$ are similarly defined as $1_{\omega_i^2}(0.01^2, 2^2)$.

Table 1 Published KETO and MDZ Data Sets

Sources	dose (mg)	sample size per subject (time frame)	Size (M/F)	meal
KETO				
Gascoigne <i>et al.</i> 1981	200 capsule	5(1 – 24h)	3(N/A)	fasting
	200 solution	5(1 – 24h)	3(N/A)	fasting
	100,200,400 tablet	8(0.5-48h)	12(N/A)	meal
	200 solution	8(0.5-48h)	12(N/A)	meal
Daneshmend <i>et al.</i> 1981	200, 400 tablet	14(0.5 – 48h)	28-44 6(6/0)	meal
Daneshmend <i>et al.</i> 1983	200 tablet, 7(0-24h)	10(0.5-8h)	8(8/0)	fasting
Daneshmend <i>et al.</i> 1984	200, 400, 600 800, tablet	13(0.5, 32h)	8(3/5) (20-31)	meal
Huang <i>et al.</i> 1986	200 solution	12(0.5-48h)	24(24/0)	fasting
	suspension, tablet 200, 400, 800 solution.	12(0.5-48h)	12(24/0)	fasting
Novopharm Ltd (FDA, 1999)	200 tablet	17(1/4-24h)	39(39/0)	fasting
	200 tablet	17(1/4-24)	23(24/0)	meal
TEVA Pharm. (FDA, 1999)	200 tablet	15(1/3-48)	24(24/0)	fasting
	200 tablet	15(1/3-48)	17(17/0)	meal
MDZ :				
Lee <i>et al.</i> 2002	2 IV fusion	27(1/2-6h)	12(6/6)	fasting
Tsunoda <i>et al.</i> 1999	2 IV	12(1/4-8h)	9(6/3)	fasting

Table 2 Pharmacokinetics Parameter Estimates for KETO and MDZ

Parameters	Methods			
	Model 2*		Model 1**	
	Estimate	90% CI***	Estimate	90% CI***
<u>KETO:</u>				
V_{1_I}	23.9	(0.86, 1.12)	21.3	(0.82, 1.22)
V_{2_I}	36.1	(0.63, 1.69)	33.8	(0.53, 1.32)
$V \max_I$	21.3	(0.90, 1.11)	22.2	(0.81, 1.21)
CL_{12_I}	2.04	(0.62, 1.59)	2.10	(0.52, 1.80)
$ka_{I, TM}$	0.48	(0.78, 1.31)	0.45	(0.73, 1.44)
$ka_{I, TF}$	0.70	(0.78, 1.31)	0.72	(0.74, 1.49)
$ka_{I, SPF}$	1.85	(0.77, 1.32)	1.79	(0.76, 1.48)
$ka_{I, SLM}$	0.80	(0.78, 1.31)	0.76	(0.76, 1.45)
$ka_{I, SLF}$	2.30	(0.77, 1.33)	2.23	(0.74, 1.49)
$\omega_{V_{1_I}}$	0.14	(0.44, 1.72)	0.13	(0.43, 2.02)
$\omega_{V_{2_I}}$	0.64	(0.51, 1.54)	0.66	(0.46, 1.73)
$\omega_{V \max_I}$	0.14	(0.58, 1.52)	0.15	(0.52, 1.70)
$\omega_{CL_{12_I}}$	0.72	(0.60, 1.47)	0.77	(0.52, 1.78)
ω_{ka_I}	0.38	(0.52, 1.53)	0.40	(0.44, 1.77)
σ_{I1}	0.49	(0.96, 1.03)	N/A	
σ_{I0}	0.10	(0.28, 1.73)	N/A	
<u>MDZ :</u>				
V_{1_S}	76.56	(0.63, 1.60)	70.05	(0.73, 1.60)
V_{2_S}	50.98	(0.60, 1.60)	49.08	(0.61, 1.66)
$V \max_S$	4757.3	(0.62, 1.60)	4488	(0.68, 1.56)
CL_{12_S}	41.38	(0.59, 1.66)	44.5	(0.55, 1.65)
ω_S	0.32	(0.62, 1.53)	0.34	(0.64, 1.55)
σ_{S1}	0.14	(0.64, 1.38)	N/A	
σ_{S0}	0.10	(0.31, 1.63)	N/A	

Note:

Model 2* : a Bayesian three-level hierarchical model for the sample mean and variance.

Model 1** : a Bayesian three-level hierarchical model for the sample mean.

90% CI*** : a 90% credit interval. It is represented by its relative scale to the mean.

Table 3 : Population-Average and Subject-Specific AUCR Prediction

<i>Ki</i>	<i>Dose/Combination</i> (KETO/MDZ)mg	Population-Average AUCR	Subject-Specific AUCR	Between- Subject/Study CV
0.0037	200/2	3.02 ×/÷ 1.112	2.94 ×/÷ 1.258	0.242 ×/÷ 1.090
0.01	200/2	2.43 ×/÷ 1.084	2.35 ×/÷ 1.222	0.217 ×/÷ 1.116
0.18	200/2	1.21 ×/÷ 1.014	1.19 ×/÷ 1.085	0.084 ×/÷ 1.078
0.0037	400/5	3.72 ×/÷ 1.130	3.50 ×/÷ 1.273	0.254 ×/÷ 1.116
0.01	400/5	3.17 ×/÷ 1.108	2.94 ×/÷ 1.255	0.234 ×/÷ 1.091
0.18	400/5	1.45 ×/÷ 1.020	1.39 ×/÷ 1.124	0.120 ×/÷ 1.066
0.0037	800/10	3.93 ×/÷ 1.139	3.61 ×/÷ 1.280	0.249 ×/÷ 1.155
0.01	800/10	3.56 ×/÷ 1.119	3.34 ×/÷ 1.260	0.224 ×/÷ 1.139
0.18	800/10	1.78 ×/÷ 1.028	1.69 ×/÷ 1.153	0.151 ×/÷ 1.058

Note: the results are presented as mean ×/÷ (1+CV)*100%.

Table 4 : Bias of PK Parameter Estimates

Parameters	True	Methods			
		Model 2*		Model 1**	
		Est.	RB%	Est.	RB%
<u><i>KETO:</i></u>					
V_{1_I}	24.0	23.3	-2.9%	23.4	-2.5%
V_{2_I}	35.0	33.4	-4.6%	33.3	-4.8%
V_{\max_I}	21.0	21.5	2.4%	21.6	2.9%
CL_{12_I}	2.0	2.15	7.5%	2.19	8.2%
ka_I	0.5	0.49	-2.0%	0.49	-2.0%
$\omega_{V_{1_I}}$	0.30	0.31	3.0%	0.30	0.8%
$\omega_{V_{2_I}}$	0.30	0.30	0.9%	0.31	3.0%
$\omega_{V_{\max_I}}$	0.30	0.31	2.6%	0.30	0.9%
$\omega_{CL_{12_I}}$	0.30	0.30	0.5%	0.31	3.0%
ω_{ka_I}	0.30	0.29	-2.9%	0.30	0.3%
σ_{I1}	0.20	0.21	5.0%	N/A	
<u><i>MDZ:</i></u>					
V_{1_S}	78	80.0	2.6%	80.2	2.8%
V_{2_S}	53	55.0	3.8%	55.3	4.3%
V_{\max_S}	4878	4934	1.1%	4954	1.6%
CL_{12_S}	43	42.1	-2.09%	42.4	-1.4%
$\omega_{V_{1_I}}$	0.30	0.30	0.0%	0.32	6.7%
$\omega_{V_{2_I}}$	0.30	0.29	-3.2%	0.30	0.0%
$\omega_{V_{\max_I}}$	0.30	0.29	-3.2%	0.31	-2.9%
$\omega_{CL_{12_I}}$	0.30	0.29	-2.4%	0.30	-0.4%
σ_{S1}	0.20	0.21	5.0%	N/A	

Note:

Model 2* : a Bayesian three-level hierarchical model for the sample mean and variance.

Model 1** : a Bayesian three-level hierarchical model for the sample mean.

Figure 1: (a) published ketoconazole studies; (b) published midazolam studies. Every curve represents a sample mean drug concentration profile; multiple curves from one study represent multiple phases of a pharmacokinetics study.

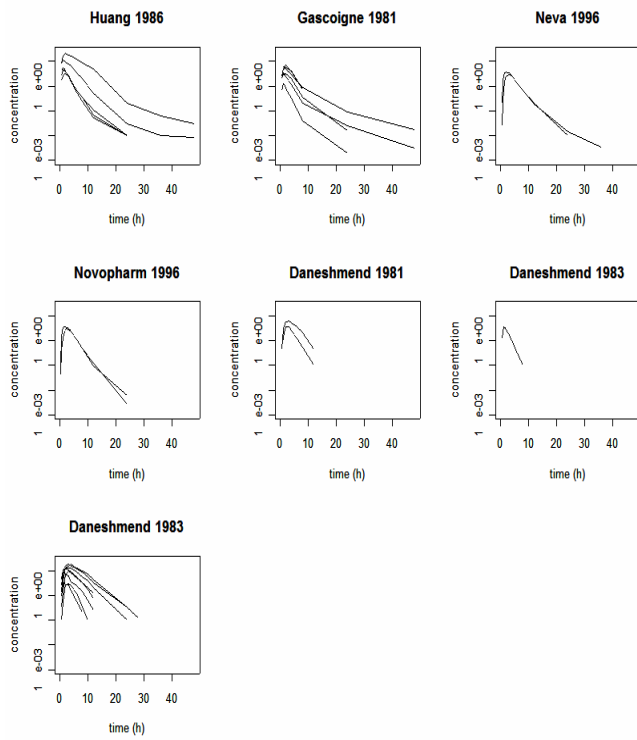
Figure 2: (a) The fitting of sample coefficient of variance from a ketoconazole study (Gascoigne *et al.* 1981). The solid line is the sample coefficient variance, and dots are the posterior draws of the predicted coefficient of variance. (b) The fitting of sample coefficient of variance from a midazolam study (Lee *et al.* 2002). The solid line is the sample coefficient variance, and dots are the posterior draws of the predicted coefficient of variance.

Figure 3: (a), (b), and (c) are population-average *AUCR* prediction estimates, relative bias, and 90% credit interval coverage probability respectively. (d), (e), and (f) are subject-specific *AUCR* prediction estimates, relative bias, and 90% credit interval coverage probability respectively. These results are based on 100 simulated data sets.

Figure 4: (a), (b), and (c) are between-subject/study *AUCR* coefficient of variance estimates, relative bias, and 90% credit interval coverage probability respectively. These results are based on 100 simulated data sets.

Figure 1: Published Ketoconazole (a) and Midazolam sample mean data.

(a)



(b)

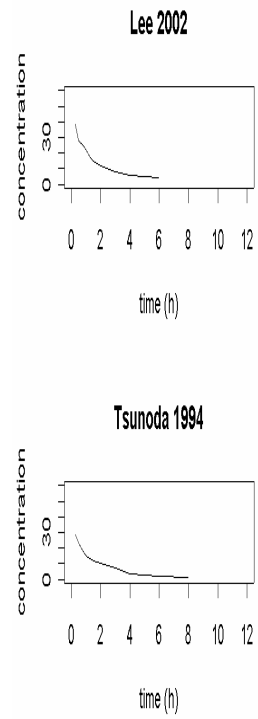


Figure 2: The Fitting of Sample Coefficient of Variation

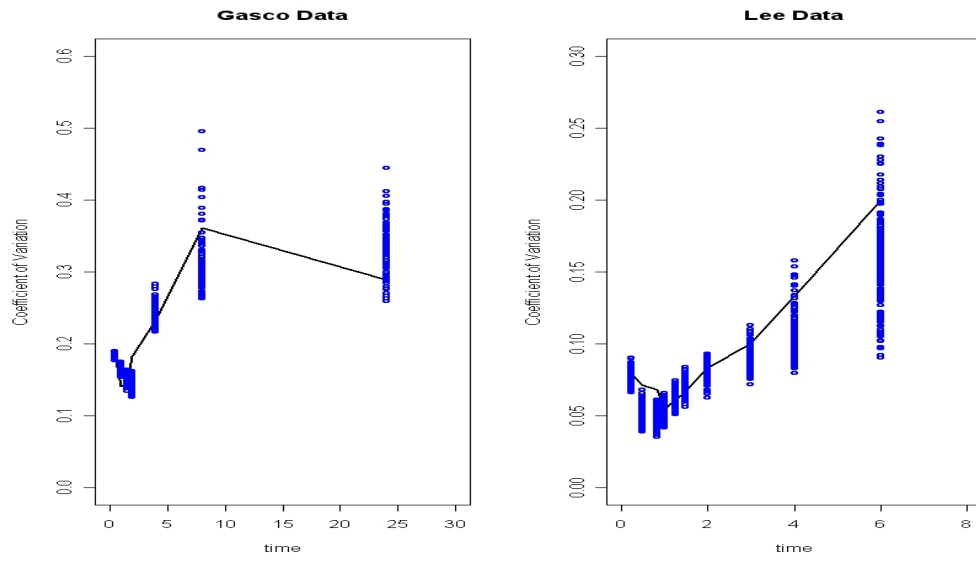


Figure 3: Bias and Coverage Probability of AUCR Predictions.

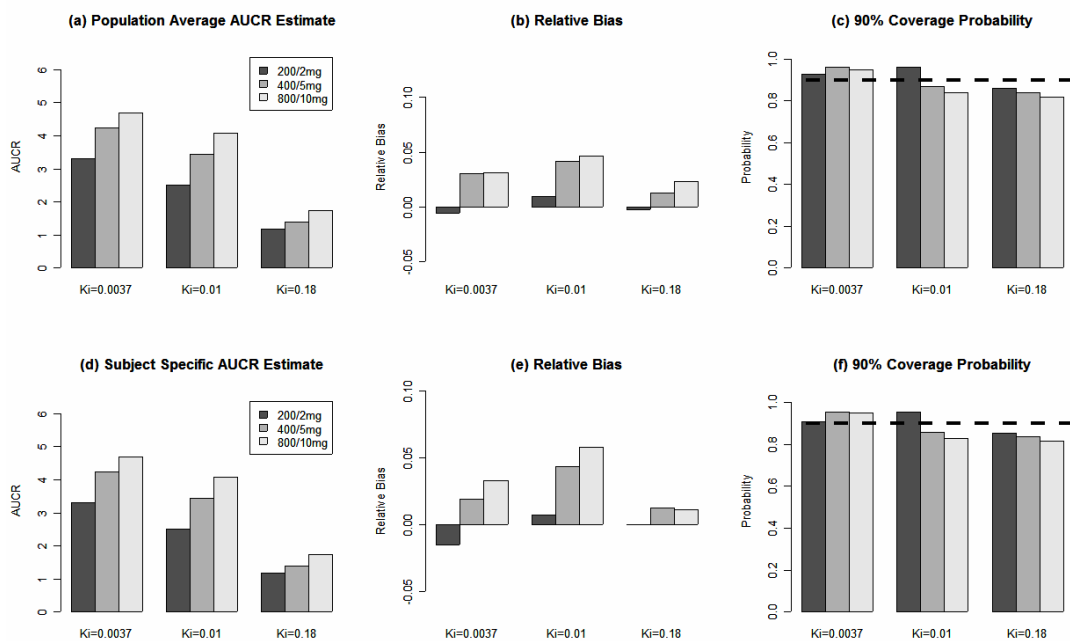


Figure 4. Bias and Coverage Probability of AUCR Coefficient of Variation Prediction

